

## Novel Bismuth and Lead Coordination Polymers Synthesized with Pyridine-2,5-Dicarboxylates: Two Single Component “White” Light Emitting Phosphors

Arief C. Wibowo, Shae A. Vaughn, Mark D. Smith, and Hans-Conrad zur Loye\*

Department of Chemistry and Biochemistry, University of South Carolina, 631 Sumter Street, Columbia, South Carolina 29208, United States

Received July 22, 2010

New two-dimensional (2D) bismuth and three-dimensional (3D) lead based coordination polymers containing pyridine-2,5-dicarboxylate ligands ( $H_2pydc$ ) have been synthesized hydrothermally and characterized by single crystal X-ray diffraction.  $Bi_3(\mu_3-O)_2(pydc)_2(Hpydc)(H_2O)_2$  (**1**), which crystallizes in the space group  $P\bar{1}$  ( $a = 8.7256(5)$  Å,  $b = 11.1217(7)$  Å,  $c = 14.0933(9)$  Å,  $\alpha = 85.239(1)^\circ$ ,  $\beta = 98.582(1)^\circ$ ,  $\gamma = 71.106(1)^\circ$ ), has a 3D structure that contains  $Bi_6O_4$  clusters that connect into 2D sheets via linking ligands. The sheets form a 3D supramolecular structure via hydrogen bonding along the  $z$ -axis.  $Pb(pydc)(H_2O)$  (**2**), which crystallizes in the space group  $P2_1/c$  ( $a = 10.8343(14)$  Å,  $b = 11.2099(15)$  Å,  $c = 6.6573(9)$  Å,  $\beta = 90.697(2)^\circ$ ), contains 1D chains of corner-sharing distorted face capped trigonal prisms that are connected into a 3D framework via the  $pydc$  ligand. In addition, the ligands are hydrogen bonded to each other. Both **1** and **2** are single component “white” light emitting phosphors and are shown to exhibit “white” luminescence that covers a much wider spectral range than is observed for the as received  $H_2pydc$  ligand.

### Introduction

The development of white-light-emitting diodes (WLEDs) is an important target of solid-state lighting research, as these materials, coupled with the appropriate phosphors, offer long lifetime, significant energy savings, and are on track to replace existing mercury containing fluorescent lights.<sup>1</sup> The visual perception of white light in today’s fluorescent light bulbs is created by a combination of broad intensity distribution and narrow band-emission light sources.<sup>2</sup> Specifically, fluorescent lights utilize a combination of mercury vapor and semiconducting phosphors to emit white composite photoluminescence. While a variety of different phosphors are used in these lights, they all rely on excitation by the main mercury emission lines at 408, 440, and 550 nm.<sup>2</sup> Environmental concerns raised by the extensive use of mercury is motivating the search for safer and, at the same time, more energy efficient LED-based solid-state lights. To date, different approaches have been reported to develop efficient WLEDs, all of which rely on utilizing a combination of colored phosphors. The ability to use a single “white” light emitting phosphor clearly would be advantageous.

Metal–organic hybrid materials are attractive materials for a variety of applications ranging from heterogeneous catalysis, nonlinear optical properties, ion exchange behavior,

selective adsorption behavior, potential quantum dot behavior, advanced gas storage capabilities, ferro- and/or piezoelectricity, to luminescence properties.<sup>3–14</sup> Polydentate ligands play a crucial role in the self-assembly of coordination polymers during solvothermal synthesis. In particular, aromatic dicarboxylic acid based ligands are well-known for their utility in the preparation of novel framework materials for potential application in gas storage,<sup>15–18</sup> magnetic,<sup>19</sup> and luminescent properties.<sup>20–23</sup> Typically, these ligands are reacted with

- (3) Evans, O. R.; Lin, W. *Acc. Chem. Res.* **2002**, *35*, 511.
- (4) Kitagawa, S.; Kitaura, R.; Shin-ichiro, N. *Angew. Chem., Int. Ed.* **2004**, *43*, 2334.
- (5) Miller, J. *Adv. Mater.* **2001**, *13*, 525.
- (6) Proserpio, D.; Hoffman, R.; Preuss, P. *J. Am. Chem. Soc.* **1994**, *116*, 9634.
- (7) Rao, C. N. R.; Natarajan, S.; Vaidhyanathan, R. *Angew. Chem., Int. Ed.* **2004**, *43*, 1466.
- (8) Reineke, T. M.; Eddaoudi, M.; Moler, D.; O’Keeffe, M.; Yaghi, O. M. *J. Am. Chem. Soc.* **2000**, *122*, 4843.
- (9) Rowsell, J.; Yaghi, O. *Microporous Mesoporous Mater.* **2004**, *73*, 3.
- (10) Sauvage, J. *Acc. Chem. Res.* **1998**, *31*, 611.
- (11) Seo, J.; Whang, D.; Lee, H.; Jum, S.; Oh, J.; Jeon, Y.; Kim, K. *Nature*. **2000**, *404*, 982.
- (12) Yaghi, O.; Keffe, M. O.; Ockwig, N.; Chae, H.; Eddaoudi, M.; Kim, J. *Nature*. **2003**, *423*, 705.
- (13) Zhang, W.; Ye, H.-Y.; Xiong, R.-G. *Coord. Chem. Rev.* **2009**, *253*, 2980.
- (14) Yu, X.; Zhang, H.; Cao, Y.; Chen, Y.; Wang, Z. *J. Solid State Chem.* **2006**, *179*, 247.
- (15) Hong, D.-Y.; Hwang, Y. K.; Serre, C.; Ferey, G.; Chang, J.-S. *Adv. Funct. Mater.* **2009**, *19*, 1537.
- (16) Bauer, S.; Serre, C.; Devic, T.; Horcajada, P.; Marrot, J.; Ferey, G.; Stock, N. *Inorg. Chem.* **2008**, *47*, 7568.
- (17) Ferey, G.; Mellot-Drznieks, C.; Serre, C.; Millange, F.; Dutour, J.; Surlbe, S.; I, M. *Science*. **2005**, *309*, 2040.

\*To whom correspondence should be addressed. E-mail: zurloye@mail.chem.sc.edu.

(1) Liu, R.-S.; Drozd, V.; Bagkar, N.; Shen, C.-C.; Baginskiy, I.; Chen, C.-H.; Tan, C. H. *J. Electrochem. Soc.* **2008**, *155*, 71.  
(2) Fuchs, E. C.; Gatterer, K. *Cent. Eur. J. Chem.* **2008**, *6*, 497.

transition elements and, in particular, with the post-transition element zinc, where many new structural concepts have been discovered. Comparatively little work, however, has been done in the area of main group based coordination polymers, even though elements such as bismuth, tin, lead, and antimony coordinate well to alkoxide and/or carboxylic acids.<sup>21–31</sup>

We are interested in exploring coordination polymers containing main group metals that possess stereochemically active lone pairs ( $ns^2np^0$  electron configuration) such as lead and bismuth. Despite the environmental concern of lead, lead-based coordination polymer research has started to attract more attention because of lead's flexible coordination environments and the potential of observing cooperative effects due to lead's stereochemically active lone pair, which can lead both to interesting structures and luminescence properties.<sup>21–23</sup> In the world of oxide chemistry, the presence of stereochemically active lone pairs in an oxide can lead to non-centrosymmetric structures possessing optical activity and ferro- and/or piezo-electricity.<sup>32</sup>

Bismuth-containing compounds with their low toxicity, low cost, and good chemical stability,<sup>33–35</sup> show promise for potential applications in medical treatment, catalysts, and luminescence.<sup>36–39</sup> The ability of bismuth to exist in a wide range of coordination environments makes it especially attractive as a flexible metal in the field of coordination chemistry. In particular the combination of a rigid linking ligand such as pyridine-2,5-dicarboxylic acid ( $H_2pydc$ ), Scheme 1, with a metal possessing a flexible coordination sphere, such as bismuth, can lead to new and interesting structural motifs. The limited solubility of bismuth salts, however, has made the preparation of bismuth(III) coordination compounds a challenge and, perhaps for this reason, bismuth based framework materials are relatively rare when compared to those of other

**Scheme 1.** Structure of Pyridine-2,5-dicarboxylic Acid ( $H_2pydc$ )

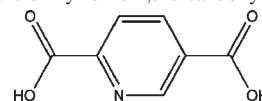


**Table 1.** Crystal Data and Structure Refinement of Compounds 1 and 2

	1	2
empirical formula	$C_{21}H_{14}Bi_3N_3O_{16}$	$C_7H_5N O_5Pb$
formula weight	1191.29	390.31
temperature	295(2) K	295(2) K
wavelength	0.71073 Å	0.71073 Å
crystal system	triclinic	monoclinic
space group	$P\bar{1}$	$P2_1/c$
unit cell dimensions		
<i>a</i> , Å	8.7256(5)	10.8343(14)
$\alpha$ , deg	85.239(1)	90
<i>b</i> , Å	11.1217(7)	11.2099(15)
$\beta$ , deg	84.843(1)	90.697(2)
<i>c</i> , Å	14.0933(9)	6.6573(9)
$\gamma$ , deg	71.106(1)	90
volume, Å <sup>3</sup>	1286.63(14)	808.48(19)
<i>Z</i>	2	4
density (calculated)	3.075 Mg/m <sup>3</sup>	3.207 Mg/m <sup>3</sup>
absorption coefficient	20.554 mm <sup>-1</sup>	20.862 mm <sup>-1</sup>
<i>F</i> (000)	1076	704
crystal size	0.05 × 0.04 × 0.02 mm <sup>3</sup>	0.08 × 0.05 × 0.02 mm <sup>3</sup>
$\theta$ range for data collection	1.45 to 26.41°	1.88 to 26.37°
index ranges	−10 ≤ <i>h</i> ≤ 10 −13 ≤ <i>k</i> ≤ 13 −17 ≤ <i>l</i> ≤ 17	−13 ≤ <i>h</i> ≤ 13 −14 ≤ <i>k</i> ≤ 14 −8 ≤ <i>l</i> ≤ 8
reflections collected	22885	10425
independent reflections	5268 [ <i>R</i> (int) = 0.0518]	1656 [ <i>R</i> (int) = 0.0571]
completeness to $\theta$	99.7%	100.0%
absorption correction	semiempirical from equivalents	semiempirical from equivalents
max. and min transmission	1.0000 and 0.5304	1.0000 and 0.5426
refinement method	full-matrix least-squares on $F^2$	full-matrix least-squares on $F^2$
data/restraints/parameter	5268/2/391	1656/3/133
goodness-of-fit on $F^2$	1.014	1.028
final <i>R</i> indices	<i>R</i> 1 = 0.0307	<i>R</i> 1 = 0.0288
[ <i>I</i> > 2 $\sigma$ ( <i>I</i> )]	<i>wR</i> 2 = 0.0636 <i>R</i> 1 = 0.0391	<i>wR</i> 2 = 0.0559 <i>R</i> 1 = 0.0396
<i>R</i> indices (all data)	<i>wR</i> 2 = 0.0671	<i>wR</i> 2 = 0.0593
largest diff. peak and hole	1.569 and −0.933 e Å <sup>-3</sup>	1.300 and −0.719 e Å <sup>-3</sup>

(18) Serre, C.; Bourrelly, S.; Vimont, A.; Ramsahye, N. A.; Maurin, G.; Llewellyn, P. L.; Daturi, M.; Filinchuk, Y.; Leynaud, O.; Barnes, P.; Ferey, G. *Adv. Mater.* **2007**, *19*, 2246.

(19) Huang, Y.-G.; Wang, X.-T.; Jiang, F.-L.; Gao, S.; Wu, M.-Y.; Gao, Q.; Wei, W.; Hong, M.-C. *Chem.—Eur. J.* **2008**, *14*, 10340.

(20) Chi, Y.-X.; Niu, S.-Y.; Jin, J. *Inorg. Chim. Acta* **2009**, *362*, 3821.

(21) Zhao, Y.-H.; Xu, H.-B.; Fu, Y.-M.; Shao, K.-Z.; Yang, S.-Y.; Su, Z.-M.; Hao, X.-R.; Zhu, D.-X.; Wang, E.-B. *Cryst. Growth Des.* **2008**, *8*, 3566.

(22) Wang, X.-L.; Chen, Y.-Q.; Gao, Q.; Lin, H.-Y.; Liu, G.-C.; Zhang, J.-X.; Tian, A.-X. *Cryst. Growth Des.* **2010**, *10*, 2174.

(23) Li, C.-P.; Yu, Q.; Chen, J.; Du, M. *Cryst. Growth Des.* **2010**, *10*, 2650.

(24) Tan, Y.-X.; Meng, F.-Y.; Wu, M.-C.; Zeng, M.-H. *J. Mol. Struct.* **2009**, *928*, 176.

(25) Davidovich, R. L.; Stavila, V.; Marinin, D. V.; Voit, E. I.; Whitmire, K. H. *Coord. Chem. Rev.* **2009**, *253*, 1316.

(26) Wang, X.; Liu, L.; Makarenko, T.; Jacobson, A. J. *Cryst. Growth Des.* **2010**, *10*, 1960.

(27) Thirumurugan, A.; Tan, J.-C.; Cheetham, A. K. *Cryst. Growth Des.* **2010**, *10*, 1736.

(28) James, S. C.; Norman, N. C.; Orpen, A. G.; Quayle, M. J.; Weckenmann, U. *J. Chem. Soc., Dalton Trans.* **1996**, 4159.

(29) Jolas, J. L.; Hoppe, S.; Whitmire, K. H. *Inorg. Chem.* **1997**, *36*, 3335.

(30) Whitmire, K. H.; Hoppe, S.; Sydor, O.; Jolas, J. L.; Jones, C. M. *Inorg. Chem.* **2000**, *39*, 85.

(31) Stavila, V.; Whitmire, K. H.; Rusakova, I. *Chem. Mater.* **2009**, *21*, 5456.

(32) Halasyamani, P. S.; Poepplmeier, K. R. *Chem. Mater.* **1998**, *10*, 2753.

(33) Suzuki, H.; Matano, Y. *Organobismuth Chemistry*; Elsevier B. V.; Amsterdam, 2001.

(34) Gaspard-Illoughmane, H.; Le Roux, C. *Eur. J. Org. Chem.* **2004**, *2004*, 2517.

(35) Leonard, N. M.; Wieland, L. C.; Mohan, R. S. *Tetrahedron.* **2002**, *58*, 8373.

(36) Sun, H.; Sadler, P. *Top. Biol. Inorg. Chem.* **1999**, *2*, 159.

(37) Repichet, S.; Le Roux, C.; Dubac, J.; Desmurs, J.-R. *Eur. J. Org. Chem.* **1998**, 2743.

(38) Leonard, N. M.; Oswald, M. C.; Freiberg, D. A.; Nattier, B. A.; Smith, R. C.; Mohan, R. S. *J. Org. Chem.* **2002**, *67*, 5202.

(39) Nikol, H.; Vogler, A. *J. Am. Chem. Soc.* **1991**, *113*, 8988.

metals.<sup>28–31,40–43</sup> However, some reflux slow-cool processes have led to the formation of bismuth based coordination polymer, such as the recent work by Anjaneyulu et al. who have reported on Bi(III) complexes made with picolinic acid, dipicolinic acid, and quinaldic acid.<sup>44</sup>

We have explored the use of pyridine-2,5-dicarboxylic acid in the preparation of new main group metal containing coordination polymers. Herein we report the hydrothermal synthesis of new 2D bismuth and 3D lead containing

(40) Greenwood, N. N.; Earnshaw, A. *Chemistry of the Elements*; Pergamon Press: Oxford, 1984.

(41) Wilkinson, G.; Gillard, R. D.; McCleverty, J. A. *Comprehensive Coordination Chemistry*; Pergamon: London, 1987.

(42) Bondi, A. *J. Chem. Phys.* **1964**, *68*, 441.

(43) Rogers, R. D.; Bond, A. H. *J. Am. Chem. Soc.* **1992**, *114*, 2960.

(44) Anjaneyulu, O.; Prasad, T. K.; Swamy, K. C. K. *Dalton Trans.* **2010**, *39*, 1935.

**Table 2.** Representative Bond Lengths (Å) of Compound 1<sup>a</sup>

Bi(1)–O(13)	2.110(4)	Bi(3)–O(14)	2.095(5)
Bi(1)–O(1)	2.292(5)	Bi(3)–O(13)	2.234(5)
Bi(1)–O(7)#1	2.342(5)	Bi(3)–O(10)	2.350(5)
Bi(1)–O(6)#2	2.545(5)	Bi(3)–O(5)	2.460(5)
Bi(1)–N(1)	2.638(6)	Bi(3)–O(15)	2.632(6)
Bi(1)–O(12)#3	2.685(5)	Bi(3)–N(2)	2.679(6)
Bi(1)–N(3)#3	2.843(6)	Bi(3)–O(1)	3.006(5)
Bi(1)–O(8)#1	2.955(5)	Bi(3)–O(16A)	3.07(2)
Bi(1)–O(5)#2	3.112(5)	N(3)–Bi(1)#3	2.843(6)
Bi(2)–O(14)	2.107(5)	O(4)–H(4A)	0.847(10)
Bi(2)–O(13)	2.182(5)	O(5)–Bi(1)#6	3.112(5)
Bi(2)–O(11)#4	2.289(5)	O(6)–Bi(1)#6	2.545(5)
Bi(2)–O(9)	2.380(5)	O(7)–Bi(1)#7	2.342(5)
Bi(2)–O(14)#5	2.383(4)	O(8)–Bi(1)#7	2.955(5)
Bi(2)–O(12)#4	3.172(6)	O(11)–Bi(2)#8	2.289(5)
Bi(2)–Bi(3)	3.4192(4)	O(12)–Bi(2)#8	3.172(6)
Bi(2)–Bi(2)#5	3.6980(5)	O(14)–Bi(2)#5	2.382(4)
Bi(2)–Bi(3)#5	4.1959(4)		

<sup>a</sup> Symmetry transformations used to generate equivalent atoms: #1  $x, y+1, z$  #2  $x+1, y, z$  #3  $-x+1, -y+2, -z+1$  #4  $x+1, y-1, z$  #5  $-x+1, -y+1, -z+1$  #6  $x-1, y, z$  #7  $x, y-1, z$  #8  $x-1, y+1, z$ .

**Table 3.** Representative Bond Lengths (Å) for Compound 2<sup>a</sup>

Pb(1)–O(5)	2.445(5)
Pb(1)–O(3)#1	2.453(6)
Pb(1)–O(1)	2.516(5)
Pb(1)–N(1)	2.517(6)
Pb(1)–O(2)#2	2.789(5)
Pb(1)–O(2)#3	2.902(5)
Pb(1)–O(4)#4	2.917(5)
O(3)–Pb(1)#5	2.453(6)
O(5)–H(5A)	0.842(15)
O(5)–H(5B)	0.846(15)

<sup>a</sup> Symmetry transformations used to generate equivalent atoms: #1  $-x+1, y+1/2, -z+3/2$  #2  $-x, y+1/2, -z+3/2$  #3  $-x, -y+1, -z+2$  #4  $-x+1, -y+1, -z+2$  #5  $-x+1, y-1/2, -z+3/2$ .

coordination polymers,  $\text{Bi}_3(\mu_3\text{-O})_2(\text{pydc})_2(\text{Hpydc})(\text{H}_2\text{O})_2$  (**1**) and  $\text{Pb}(\text{pydc})(\text{H}_2\text{O})$  (**2**), along with their structural characterization and the interesting observation of “white” luminescent properties.

## Experimental Section

All chemicals were of reagent grade and used without further purification.  $\text{Bi}(\text{NO}_3)_3 \cdot 5\text{H}_2\text{O}$  and pyridine-2,5-dicarboxylic acid, and *trans*-1,2-bis(4-pyridyl)ethylene were purchased from Sigma-Aldrich, and  $\text{Pb}(\text{NO}_3)_2$  was purchased from J. T. Baker. Elemental analyses were performed by Robertson Microlit Laboratories (Madison, NJ).

**Synthesis of  $\text{Bi}_3(\mu_3\text{-O})_2(\text{pydc})_2(\text{Hpydc})(\text{H}_2\text{O})_2$  (**1**).** A mixture of  $\text{Bi}(\text{NO}_3)_3 \cdot 5\text{H}_2\text{O}$  (0.242 g, 0.50 mmol), an excess of pyridine-2,5-dicarboxylic acid ( $\text{H}_2\text{pydc}$ ) (0.142 g, 0.85 mmol), and *trans*-1,2-bis(4-pyridyl)ethylene (0.154 g, 0.85 mmol) for pH control, in  $\text{H}_2\text{O}$  (25 mL) was sealed in a Teflon-lined bomb and heated to a temperature of 140 °C for 3 days, then cooled slowly at 0.1 °C/min to room temperature. Colorless, plate-like crystals and white polycrystalline powder were obtained in quantitative yield based on bismuth. The products were washed with dimethylformamide (DMF) to dissolve and remove any unreacted ligand. The final product was isolated by vacuum filtration. Anal. Calcd (Found) for  $\text{C}_{21}\text{H}_{14}\text{Bi}_3\text{N}_3\text{O}_{16}$ : C, 21.16 (21.51); H, 1.18 (1.22); N, 3.53 (3.65).

**Synthesis of  $\text{Pb}(\text{pydc})(\text{H}_2\text{O})$  (**2**).** A mixture of  $\text{Pb}(\text{NO}_3)_2$  (0.165 g, 0.50 mmol) and an excess of pyridine-2,5-dicarboxylic acid ( $\text{H}_2\text{pydc}$ ) (0.284 g, 1.70 mmol) in  $\text{H}_2\text{O}$  (25 mL) was sealed in a Teflon-lined bomb and heated to a temperature of 180 °C for 3 days, then cooled slowly at 0.1 °C/min to room temperature. Colorless, plate-like crystals and white polycrystalline powder were obtained in

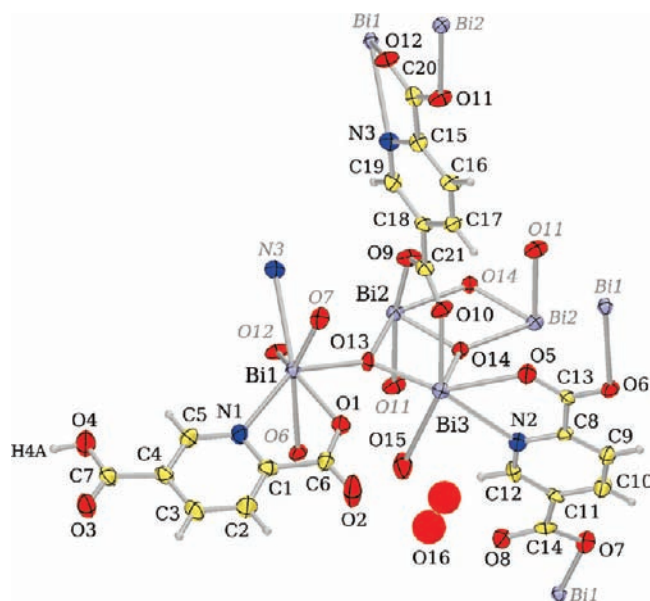


**Figure 1.** Asymmetric unit of **1** with additional symmetry-equivalent atoms (grayed labels) to complete coordination spheres. Displacement ellipsoids drawn at the 50% probability level.

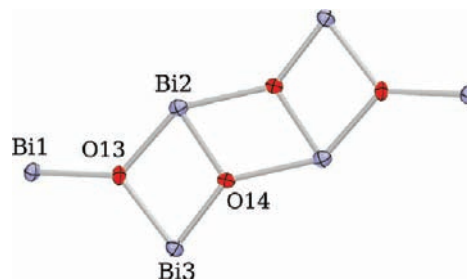


**Figure 2.** Centrosymmetric  $\text{Bi}_6\text{O}_4$  clusters of compound **1** which contains two  $\mu_3$ -oxide ligands.

quantitative yield based on lead. The products were washed with DMF to dissolve and remove any unreacted ligand. The final product was isolated by vacuum filtration. Anal. Calcd (Found) for  $\text{C}_7\text{H}_5\text{NO}_5\text{Pb}$ : C, 21.53 (21.90); H, 1.29 (1.28); N, 3.59 (3.68).

**X-ray Crystallography.** X-ray intensity data from colorless plate crystals were measured at 295(2) K using a Bruker SMART APEX diffractometer (Mo  $K\alpha$  radiation,  $\lambda = 0.71073$  Å).<sup>45</sup> Raw area detector data frame processing was performed with the SAINT+ and SADABS programs.<sup>45</sup> Final unit cell parameters were determined by least-squares refinement of 5701 (1) and 2722 (2) reflections from the data sets. Direct methods structure solution, difference Fourier calculations, and full-matrix least-squares refinement against  $F^2$  were performed with SHELXTL.<sup>46</sup>

Compound **1** crystallizes in the triclinic system. The space group  $P\bar{1}$  was confirmed by the successful solution and refinement of the structure. The asymmetric unit consists of three bismuth ions, two  $\mu_3$ -oxide ligands, three dicarboxylate ligands, and one coordinated and one uncoordinated water molecule. The uncoordinated water is disordered over two closely separated positions. One of the dicarboxylate ligands must be protonated for crystal electroneutrality. A reasonable position for a

(45) SMART Ver. 5.630, SAINT+ Ver. 6.45 and SADABS Ver. 2.10; Bruker Analytical X-ray Systems, Inc: Madison, WI, 2003.

(46) Sheldrick, G. M. SHELXTL, Version 6.14; Bruker Analytical X-ray Systems, Inc: Madison, WI, 2003.

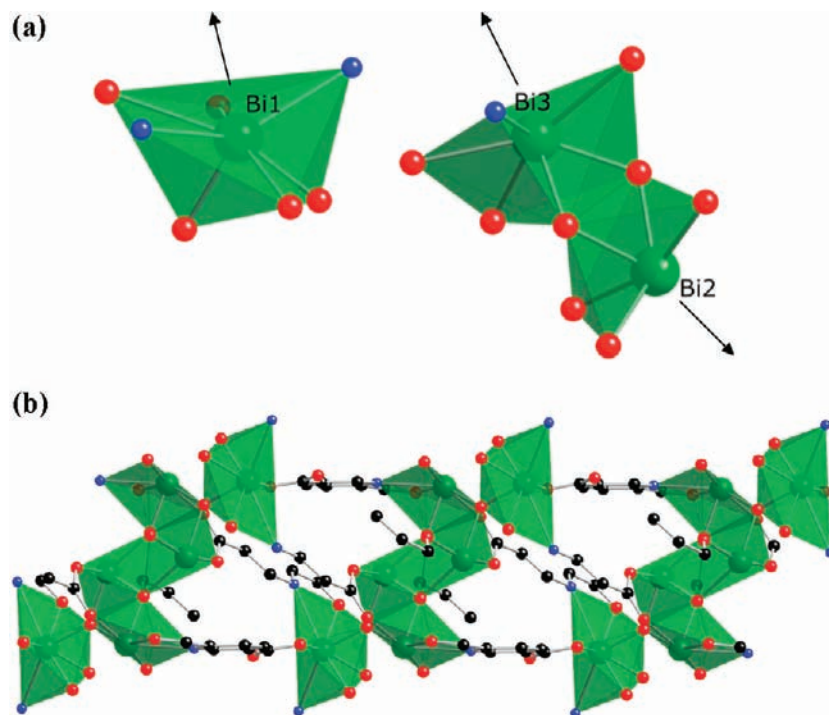


**Figure 3.** (a) Stereochemically active lone pair formation of compound **1**, the arrows show the approximate location of lone pair electrons. Bi = green, O = red, N = blue. (b) Coordination environment around bismuth in  $\text{Bi}_6\text{O}_4$  clusters of compound **1**. Bi = green, O = red, N = blue, C = black.

hydrogen atom bonded to the carboxylic oxygen O4 (H4A) was located in a difference map. Good evidence for this correctness of this hydrogen position is the formation of a classic carboxylic acid hydrogen bond between two symmetry-equivalent carboxylic acid groups. The proposed H4A position also correlates with the longer C(7)–O(4) distance. H4A was refined with O–H distance restraints and  $U_{\text{iso,H}} = 1.5(U_{\text{eq,O}})$ . All non-hydrogen atoms were refined with anisotropic displacement parameters except for the disordered water (isotropic). Hydrogen atoms bonded to carbon were placed in geometrically idealized positions and included as riding atoms. Hydrogen atoms for the coordinated and uncoordinated water molecules could not be found and were not calculated.

Compound **2** crystallizes in the space group  $P2_1/c$  as determined by the pattern of systematic absences in the intensity data. The asymmetric unit consists of one lead atom, one ligand and one water molecule. All non-hydrogen atoms were refined with anisotropic displacement parameters. Hydrogen atoms bonded to carbon were placed in geometrically idealized positions and included as riding atoms. The water hydrogens were located in Fourier difference maps and refined with O–H and H–H distance restraints, and  $U_{\text{iso,H}} = 1.5U_{\text{eq,O}}$ .

**Powder X-ray Diffraction.** Ground mixtures of polycrystalline powders and plate crystals of both **1** and **2** were used to collect powder X-ray diffraction patterns using a Rigaku D/Max 2100 Powder Diffractometer (Cu  $K\alpha$  radiation  $\lambda = 1.5418 \text{ \AA}$ ) over the  $2\theta$  range of  $2\text{--}70^\circ$ , with a step size of  $0.02^\circ$  and a scan speed of  $0.25^\circ/\text{min}$ . The measured patterns of **1** and **2** were found to match the diffraction patterns generated by CrystalMaker 8.0 using the respective single crystal data of **1** and **2**, indicating that the sample is phase pure, and that the plate crystals and the polycrystalline powder are the same product.

**UV–vis Spectrometry.** Diffuse-reflectance spectra of ground mixtures of polycrystalline powders and plate crystals of both **1** and **2** and of as received  $\text{H}_2\text{pydc}$  were obtained using a Perkin-Elmer Lambda 35 UV/vis scanning spectrophotometer equipped with an integrating sphere. The raw data were converted from reflection to absorbance by the use of the Kubelka–Munk function.

**Photoluminescence.** Excitation and emission spectra of ground mixtures of polycrystalline powders and plate crystals of both **1** and **2** and of as received  $\text{H}_2\text{pydc}$  were recorded using a Perkin-Elmer LS 55 Fluorescence Spectrometer. In all cases the maximum in the excitation spectrum was used to generate the emission spectrum. Compounds **1** and **2** were excited at 380 and 390 nm, respectively. For the as received  $\text{H}_2\text{pydc}$  ligand an excitation wavelength of 390 nm was used. All measurements were performed at room temperature.

**Thermogravimetric Analysis.** Thermogravimetric analyses were performed using a Thermal Analysis (TA) SDT-Q600 simultaneous DTA/TGA system in an oxidizing environment. Samples were heated in flowing air to  $700^\circ\text{C}$  using a heating rate of  $10^\circ\text{C}/\text{min}$ . In addition, to check the thermal stability of the metal organic framework, compound **1** was heated to  $130^\circ\text{C}$  at heating rate of  $1^\circ\text{C}/\text{min}$  and held isothermal for 2 h to remove all the water, and then cooled to room temperature. Similarly, compound **2** was heated to  $250^\circ\text{C}$  and then cooled to room temperature.

## Results and Discussion

**Structure Description.** The reactions of pyridine-2,5-dicarboxylic acid ( $\text{H}_2\text{pydc}$ ) with  $\text{Bi}(\text{NO}_3)_3 \cdot 5\text{H}_2\text{O}$  or  $\text{Pb}(\text{NO}_3)_2$  under hydrothermal conditions resulted in air stable compounds of  $\text{Bi}_3(\mu_3\text{-O})_2(\text{pydc})_2(\text{Hpydc})(\text{H}_2\text{O})_2$  (**1**) and  $\text{Pb}(\text{pydc})(\text{H}_2\text{O})$  (**2**), respectively, whose structures were determined by single crystal X-ray diffraction. Compound **1** crystallizes in a 3D structure that contains  $\text{Bi}_6\text{O}_4$  clusters that are connected into a 2D structure via ligands that connect into a 3D supramolecular structure via hydrogen bonding in the  $z$ -direction. Compound **2** contains 1D chains of corner-sharing distorted face-capped trigonal prisms that are connected into a 3D structure by the  $\text{pydc}^{2-}$  ligand. Relevant crystallographic data from the single-crystal structure refinements for **1** and **2** are found in Table 1. Selected interatomic distances are summarized in Tables 2 and 3 for compound **1** and **2**, respectively.

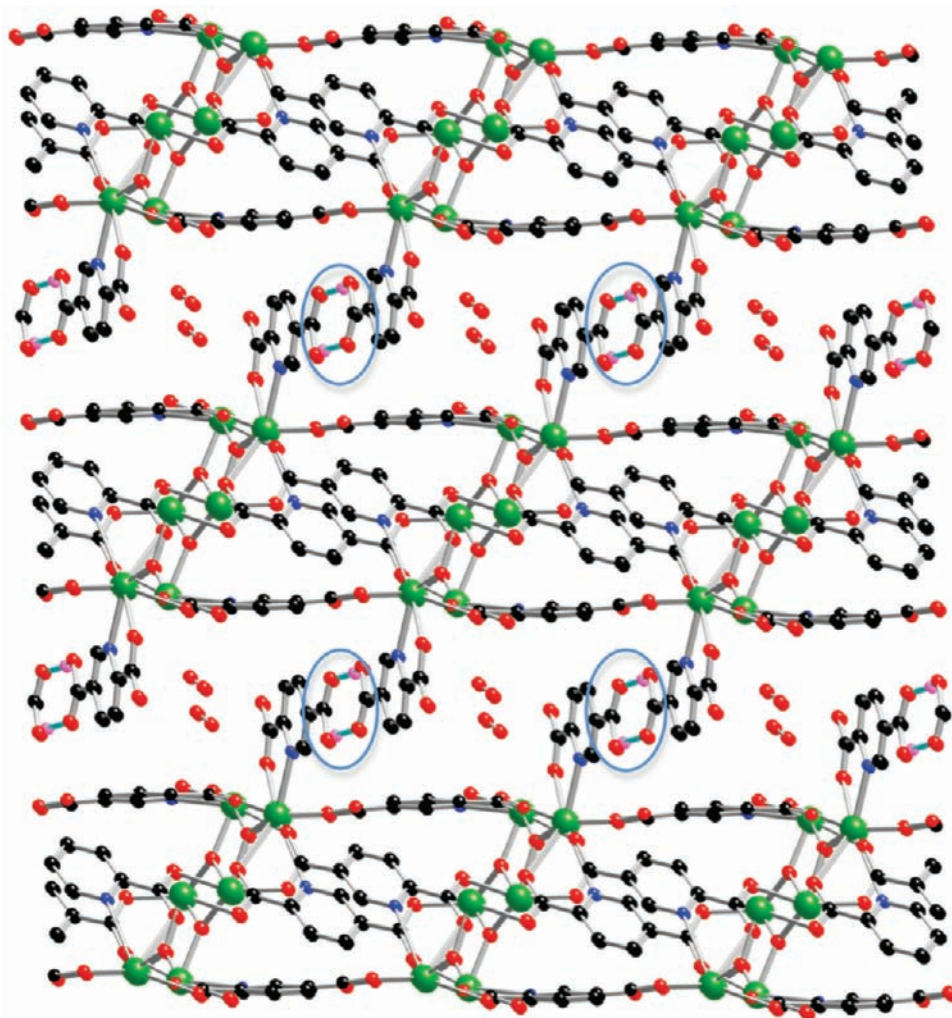


**Figure 4.** 3D structure formation of compound **1** through hydrogen bonding (light blue lines within blue circles) in  $z$ -direction. Bi = green, O = red, N = blue, C = black, H = pink.

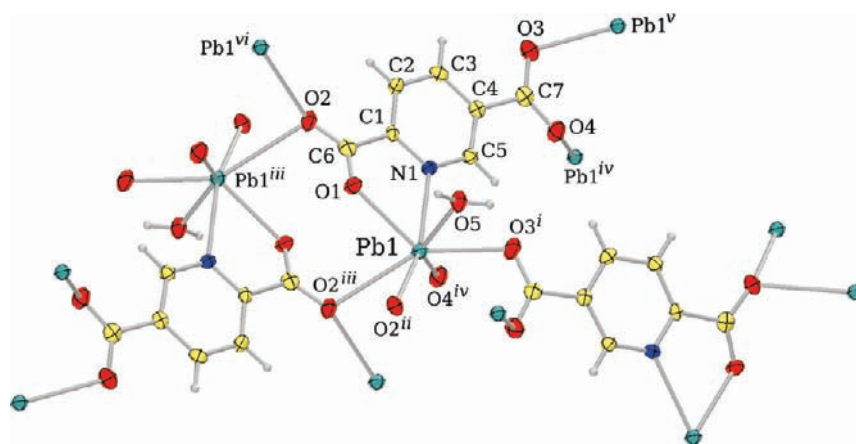


**Figure 5.** Environment of Pb(1) and the ligand (compound **2**). Displacement ellipsoids drawn at the 50% probability level. Symmetry codes: (i) =  $-x+1, y+1/2, -z+3/2$ ; (ii) =  $-x, y+1/2, -z+3/2$ ; (iii) =  $-x, -y+1, -z+2$ ; (iv) =  $-x+1, -y+1, -z+2$ ; (v) =  $-x+1, y-1/2, -z+3/2$ ; (vi) =  $-x, y-1/2, -z+3/2$ .

Figure 1 depicts the asymmetric unit cell and atom labels of  $\text{Bi}_3(\mu_3\text{-O})_2(\text{pydc})_2(\text{Hpydc})(\text{H}_2\text{O})_2$  (**1**), which consists of three bismuth ions, two  $\mu_3$ -oxide ligands, three dicarboxylato ligands, and one coordinated and one uncoordinated water molecule. The overall structure is built around centrosymmetric  $\text{Bi}_6\text{O}_4$  clusters, shown in

Figure 2, that contain the two  $\mu_3$ -oxide ligands. The nitrogen and oxygen atoms of the  $\text{pydc}^{2-}$  ligands and the oxygen atom of the coordinated water molecule complete the coordination sphere around the bismuth cations in the  $\text{Bi}_6\text{O}_4$  clusters to form  $\text{Bi}(1)\text{O}_5\text{N}_2$ ,  $\text{Bi}(2)\text{O}_5$ , and  $\text{Bi}(3)\text{O}_5\text{N}$  polyhedra, Figure 3a, with Bi–O distances ranging from

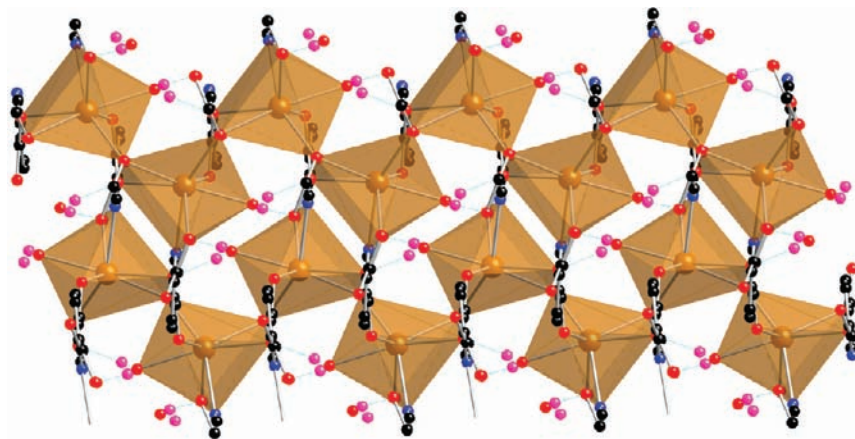
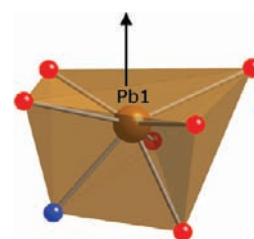


**Figure 6.** Coordination environment around lead in compound **2** showing 1D chain of  $\text{PbO}_6\text{N}$  corner-shared distorted face-capped trigonal prisms. Pb = brown, O = red, N = blue, C = black, H = pink.

2.110(4) to 2.685(5) Å, and Bi–N distances ranging from 2.638(6) to 2.843(6) Å. The distorted polyhedra contain stereochemically active lone pairs of bismuth shown in Figure 3a, where the arrows indicate the approximate location of the lone pair. The presence of stereochemically active lone pairs resulting in distorted coordination environments are commonly observed in other bismuth coordination compounds.<sup>28–31,47</sup> These polyhedra connect via the  $\text{pydc}^{2-}$  ligands to form 2D slabs that are oriented parallel to the crystallographic (110) plane in which  $\text{Bi}(2)\text{O}_5$  distorted square bipyramids share a common edge with  $\text{Bi}(3)\text{O}_5\text{N}$  distorted pentagonal pyramids, that in turn share a corner with  $\text{Bi}(1)\text{O}_5\text{N}_2$  distorted pentagonal bipyramids (Figure 3b). The 2D slabs are terminated in the third dimension by the monoprotonated  $\text{pydc}$  ( $\text{Hpydc}^-$ ) ligand (O(4)–H(4)) as shown in the Supporting Information Figure S1. This H(4) proton, shown in pink in Figure 4, is engaged in hydrogen bonding, shown as light blue lines inside blue circles, that connects the 2D slabs into the overall 3D structure. One uncoordinated water molecule that is disordered over two closely separated positions is located in between the 2D slabs.

Figure 5 depicts the asymmetric unit cell of  $\text{Pb}(\text{pydc})\cdot(\text{H}_2\text{O})$  (**2**) and contains the atom labeling scheme. The lead cation is found in a  $\text{PbO}_6\text{N}$  distorted face-capped trigonal prismatic coordination environment shown in Figure 6 with Pb–O distances ranging from 2.445(5) to 2.917(5) Å, and a Pb(1)–N(1) distance of 2.517(6) Å. Such a distorted coordination environment is indicative of a stereochemically active lone pair that appears to cap one of the two remaining faces of the trigonal prism as shown in Figure 7 where the arrow shows an approximate location of the lone pair. Similar lead-based coordination compounds are known to contain hemidirected geometries.<sup>25</sup>

Each lead polyhedron is corner shared to two neighboring polyhedra to form zigzag chains that run along the  $z$ -axis (Figure 6). The zigzag chains are connected to each other via the  $\text{pydc}^{2-}$  ligands that are oriented along the  $x$ -axis and that serve to interconnect that polyhedra into a 3D network (Figure 8 and Supporting Information



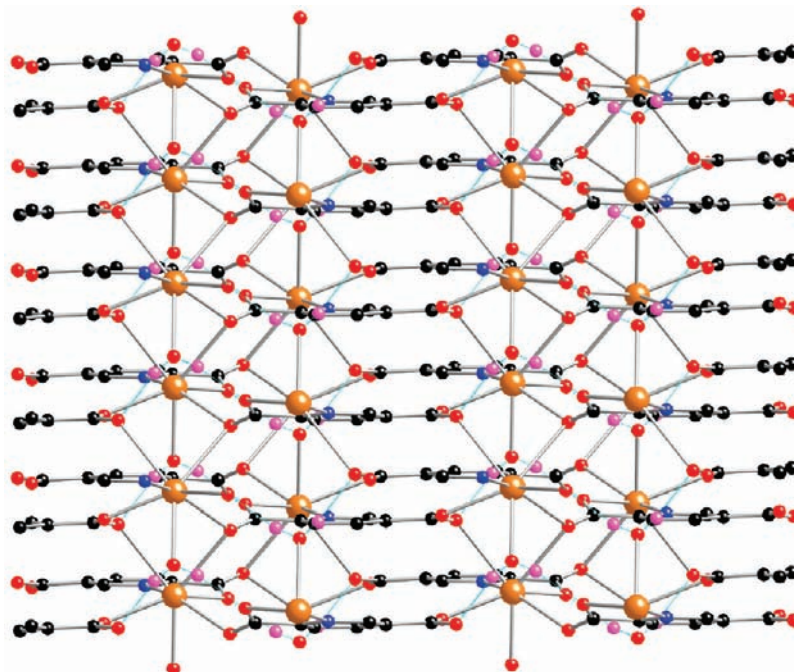
**Figure 7.** Stereochemically active lone pair formation of compound **2**, the arrow shows the approximate location of lone pair electrons. Pb = brown, O = red, N = blue.

Figure S2). In addition, there is an extensive hydrogen bonded network (shown as light blue lines) that, while reinforcing the network, is not the primary force holding the structure together. There are two types of hydrogen bonds in this structure based on the coordinated water positions as shown in Figure 8 and Supporting Information Figure S2. One is a *top-side hydrogen bond* observed between H(5)-colored in pink and O(1) as well as O(3). The other is the *bottom-side hydrogen bond* shown between H(5)-colored in pink and O(1) as well as O(4).

**Powder X-ray Diffraction.** The purity of the resulting product (mixed polycrystalline powder and ground single crystals) of compound **1** and **2** were checked using powder X-ray diffraction. While elemental analysis can provide feedback concerning the compositional content of the sample, powder X-ray diffraction can provide, in addition, phase purity information and, for example, reveal the presence or absence of polymorphs. In this case the powder diffraction patterns that were collected on ground mixtures of polycrystalline powder and plate crystals of **1** and **2**, match the calculated patterns based on the single crystal structure as shown in the Supporting Information, Figures S3 and S4 for compounds **1** and **2**, respectively. This demonstrates that the reaction products are single phases, that no additional polymorph is present, and that, within detection limits, no unreacted starting material remains in the samples used for the optical characterization.

**Thermal Analysis.** Thermogravimetric data were collected for **1** and **2** to investigate their thermal stability and to see if the water molecules present in both materials could be removed without destroying the framework. The TGA curve of compound **1** displays a gradual weight loss

(47) Asato, E.; Katsura, K.; Arakaki, T.; Mikuriya, M.; Kotera, T. *Chem. Lett.* **1994**, 2123.



**Figure 8.** 3D structure formation (in  $z$  direction) in compound **2** obtained from covalent and coordination as well as hydrogen bond (light blue lines) of pydc ligands. Pb = brown, O = red, N = blue, C = black, H = pink.

starting at  $\sim 120$  °C that persists up to  $\sim 310$  °C where a distinct weight loss step is observed. A second sharp weight loss begins at  $\sim 390$  °C. (see Supporting Information, Figure S5). The gradual weight loss appears to correspond to the loss of the uncoordinated and coordinated water molecules (observed = 4.4%, calcd 3.0%), while the distinct weight loss step at 310 °C appears to correspond to the loss of  $\text{CO}_2$  from  $\text{Hpydc}^-$  (observed = 4.1%, calcd 3.7%) and is quickly followed by a sharp weight loss at 390 °C corresponding to complete ligand decomposition (obs. 36%, calcd 33%).

Compound **2**, displays two distinct weight loss steps corresponding to the loss of the coordinated water molecule and ligand decomposition, respectively (see Supporting Information, Figure S6). The first weight loss occurs at 190 °C and corresponds to the release of water (observed = 5.1%, calcd = 4.6%). The second weight loss step occurs at 400 °C and corresponds to the decomposition of the ligand (observed = 40.7%, calcd = 42.0%).

To check the stability of the framework, compound **1** was heated to 130 °C and held isothermal for 2 h to remove all the water, and then cooled to room temperature (observed weight loss 3.2%, calcd 3.0%). A powder X-ray diffraction pattern collected on this sample indicates that the structure is still intact even after removal of all the water (see Supporting Information, Figure S7). Similarly, coordinated water of compound **2** was removed by heating to 250 °C followed by cooling to room temperature (observed weight loss 5.6%, calcd 4.6%). A powder X-ray diffraction pattern collected on this sample indicates that the structure has changed but maintained some crystallinity after removal of all the water molecules (see Supporting Information, Figure S8).

**Photoluminescence.** The luminescent properties of the coordination polymer are of interest for solid-state lighting applications, in particular in structures where the

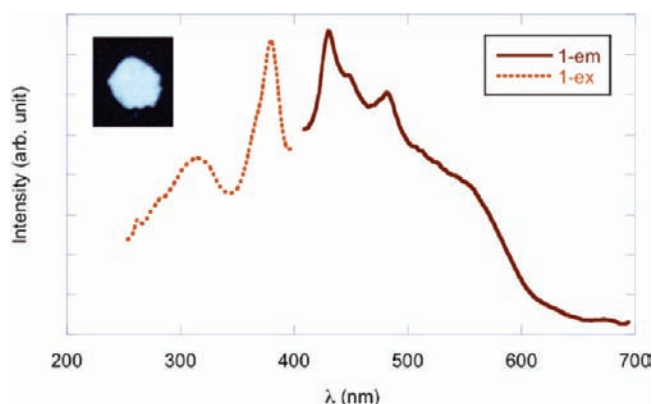


**Figure 9.** Excitation (ex; dotted line) and emission (em; solid line) spectra of compound **1**. Inset is an optical image of the “white” luminescing compound **1**.

ligand itself is luminescent, as it is possible to realize an enhancement in the intensity and a shift in the emission maxima when the ligand is incorporated into a framework structure.<sup>48</sup> The goal in solid-state lighting applications is to produce “white light”, which in reality is a complex mixture of “all” colors. For example, sunlight is considered to be “white light” and the sun’s emission spectrum, schematically shown in Supporting Information, Figure S9, starts in the UV, exhibits a maximum near 500 nm and then falls off toward the red end of the spectrum.<sup>49</sup> Light bulbs also generate a “white light” and depending on the different types of phosphors utilized, can have different hues of “white”. In all cases of white light generation, it is desirable to have a broad emission spectrum across the visible range with a peak near 500 nm.

(48) Ciurtin, D. M.; Pschirer, N. G.; Smith, M. D.; Bunz, U. H. F.; zur Loye, H.-C. *Chem. Mater.* **2001**, *13*, 2743.

(49) Rechtsteiner, G. A.; Ganske, J. A. *J. Chem. Educator* **1998**, *3*, 04230.

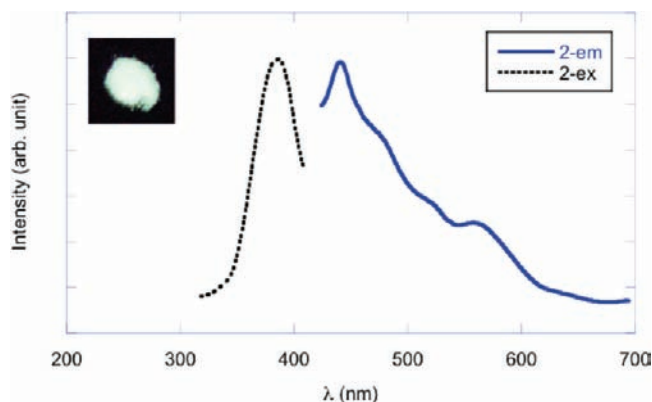


**Figure 10.** Excitation (ex; dotted line) and emission (em; solid line) spectra of compound **2**. Inset is an optical image of the “white” luminescing compound **2**.

The excitation and emission spectra of the as received  $H_2pydc$  ligand, of compound **1**, and of compound **2**, as well as their corresponding optical images representing their luminescent colors are shown in Supporting Information, Figure S10, and Figures 9 and 10, respectively. The as received  $H_2pydc$  ligand emits pale-green light with an emission maximum around 518 nm (Supporting Information, Figure S10) when excited at 390 nm. Such emission is likely due to an intraligand  $\pi \rightarrow \pi^*$  and/or  $n \rightarrow \pi^*$  transition. In contrast, the coordination polymer  $Bi_3(\mu_3-O)_2(pydc)_2(Hpydc)(H_2O)_2$  (**1**) containing the coordinated ligand exhibits “white” photoluminescence when excited at 380 nm. Specifically, compound **1** emits white composite light with a broad emission spectrum from  $\sim 400$  to  $\sim 600$  nm. Three distinct maxima at 430, 460, and 480 nm with a shoulder around 556 nm can be identified (Figure 9). Overall, the emission spectrum is significantly blue-shifted compared to the as received  $H_2pydc$  ligand, generating “white” light. The shift can be partly attributed to Ligand-to-Metal Charge Transfer (LMCT),<sup>21–23,50</sup> as well as to a change in the intraligand  $\pi \rightarrow \pi^*$  and/or  $n \rightarrow \pi^*$  transitions. The former is supported by the UV/vis spectrum of compound **1**, where a maximum absorbance is observed at 322 nm, a slight shift from the as received ligand itself, whose maximum peak is at 304 nm (Supporting Information, Figure S11). The excitation spectrum of **1** exhibits highest intensity at 380 nm (Figure 9).

Interestingly, the lead containing coordination polymer,  $Pb(pydc)(H_2O)$  (**2**) emits slightly “whiter” composite photoluminescence, very similar to what is observed for compound **1** (Figure 10), with a maximum in the UV/vis absorbance spectrum near 315 nm (Supporting Information, Figure S11). One distinct maximum is observed at 441 nm with three broad shoulders around 470, 520, and 563 nm with a similar broad emission spectrum, as shown in Figure 10. Again, the emission spectrum is blue-shifted relative to the as received  $H_2pydc$  ligand, generating “white” light. The excitation spectrum of compound **2** shows a maximum intensity at 386 nm (Figure 10).

Compound **1** retains its structure upon complete removal of the coordinated and uncoordinated water molecules and also retains its photoluminescent properties as shown in Supporting Information, Figure S12. Compound **2**, on the other hand, while maintaining crystallinity, undergoes a structural change upon water removal that is accompanied by a loss of essentially all luminescence. (see Supporting Information, Figure S13).

Similar “white” light emission from metal–organic coordination polymers was also reported by Liu et al. in their  $Zn_2Cl_4(\mu-bipy)_2$  system.<sup>1</sup> The exact mechanism for the white light emission is not understood but, in their case, was suggested to be due to the increase in ligand conformational rigidity after coordinating with zinc, which may reduce the non-radiative decay of the intraligand ( $\pi \rightarrow \pi^*$ ) excited state.<sup>1</sup> A similar ligand-based effect may also contribute to the broad emission spectra observed for our bismuth and lead coordination polymers.

It is interesting to note that bismuth-containing organic/inorganic hybrid materials have been reported to display blue luminescence,<sup>14,51,52</sup> which is quite different from the observed “white” composite emission observed for compound **1**. As for lead-based coordination compounds, recent literature shows that they can exhibit an emission spectrum that is blue-shifted relative to the ligand itself, and in some cases the emission spectra of the ligand closely resemble those of coordination complexes because of a minimal amount of shift observed.<sup>21–23</sup> The luminescent properties observed for these two coordination polymers categorize them squarely into single component “white” light emitting phosphors.

## Conclusion

We have successfully synthesized two new coordination polymers containing bismuth (a 2D coordination polymer) and lead (a 3D coordination polymer) using the pyridine-2,5-dicarboxylate ligand. Compound **1** contains  $Bi_6O_4$  clusters that are connected into 2D slabs via the ligands, which then form a 3D supramolecular structure via hydrogen bonding along the  $z$ -direction. Compound **2** contains 1D chains of corner-shared distorted capped trigonal prisms that are connected into a 3D structure via the ligand, which is also involved in extensive hydrogen bonding in the framework. Both compounds are single component “white” light emitting phosphors that make them attractive luminescent materials for solid-state lighting applications as “white” light sources.

**Acknowledgment.** Financial support for this research was provided in part by the United States Air Force award No. FA9550-08-10377 and in part by National Science Foundation through Grant CHE-0714439.

**Supporting Information Available:** Further details are given in Figures S1–S13. Crystallographic data is given in CIF format. This material is available free of charge via the Internet at <http://pubs.acs.org>.

(50) Zheng, S.-L.; Yang, J.-H.; Yu, X.-L.; Chen, X.-M.; Wong, W.-T. *Inorg. Chem.* **2004**, *43*, 830.

(51) Srivastava, A. M.; Beers, W. W. *J. Lumin.* **1999**, *81*, 293.

(52) Folkerts, H. F.; Zuidema, J.; Blasse, G. *Chem. Phys. Lett.* **1996**, *249*, 59.